NASA Grant Report
GTRI Report A5004/2000-5

Sound Absorption of a 2DOF Resonant Liner with Negative Bias Flow

K. K. Ahuja, P. Cataldi, and R. J. Gaeta, Jr.
Georgia Institute of Technology, GTRI/ATASL
Acoustics and Aerospace Technologies Branch
Atlanta, Georgia 30332-0844

Grant NAG1-1734

31 March 2000

Submitted to :

National Aeronautics and
Space Administration
Langley Research Center
Hampton, Virginia 23681-0001

Foreword/Acknowledgments

This report was prepared by the Acoustics and Aerospace Technologies Branch of the Aerospace, Transportation, and Advanced Systems Laboratory (ATASL) of Georgia Tech Research Institute (GTRI) for NASA Langley Research Center, Hampton, Virginia, under Grant NAG1-1734.

Mr. Mike Jones was the Project Manager for NASA Langley Research Center. GTRI's Project Director was Dr. K. K. Ahuja.

The authors would like to thank Mr. Tony Parrott and Mr. Mike Jones of NASA Langley Research Center for their support of this work.

Note that this report is one of five separate volumes prepared to document the work conducted by GTRI under NASA Grant NAG1-1734. The GTRI report numbers, authors, and titles of each report are listed in the table below:

GTRI Report Number	Authors	Title
A5004/2000-1	Ahuja, K. K. and Gaeta, R. J.	Active Control of Liner Impedance by Varying Perforate Orifice Geometry
A5004/2000-2	Ahuja, K. K., Munro, S. E. and Gaeta, R. J.	Flow Duct Data for Validation of Acoustic Liner Codes for Impedance Eduction
A5004/2000-3	Ahuja, K. K., Gaeta, R. J. and D'Agostino, M. S.	High Amplitude Acoustic Behavior of a Slit-Orifice backed by a Cavity
A5004/2000-4	Ahuja, K. K., Gaeta, R. J. and D'Agostino, M. S.	Acoustic Absorption Characteristics of an Orifice With a Mean Bias Flow
A5004/2000-5	Ahuja, K. K., Cataldi, P. and Gaeta, R. J.	Sound Absorption of a 2DOF Resonant Liner with Negative Bias Flow

Table of Contents

List of Figures

Executive Summary

This report describes an experimental study conducted to determine the effect of negative bias flow on the sound absorption of a two degree-of-freedom liner. The backwall for the liner was designed to act as a double-Helmholtz resonator so as to act as a hard wall at all frequencies except at its resonant frequencies. All normal incident impedance data presented herein was acquired in an impedance tube. The effect of bias flow is investigated for a buried septum porosity of 2% and 19.5% for bias flow orifice Mach numbers up to 0.311. As a porous backwall is needed for the flow to pass through, the effect of bias flow on this backwall had to be evaluated first. The bias flow appears to modify the resistance and reactance of the backwall alone at lower frequencies up to about 2 kHz, with marginal effects at higher frequencies. Absorption coefficients close to unity are achieved for a frequency range of 500- 4000 Hz for the overall liner for a septum porosity of 2% and orifice Mach number of 0.128. Insertion loss tests performed in a flow duct facility for grazing flow Mach numbers up to 0.2 and septum Mach numbers up to 0.15 showed that negative bias flow can increase insertion loss by as much as 10 dB at frequencies in the range of 500 – 1400 Hz compared to no grazing flow. The effectiveness of the negative bias flow is diminished as the grazing flow velocity is increased.

1.0 Introduction

Designing an acoustic liner with controllable wall impedance has many engineering applications. Acoustic treatment for jet engines where changing engine operating conditions necessarily change the character of the noise source is one example. Other examples include acoustic mufflers for internal combustion engines, where changing engine power levels change the noise source frequency.

Two methods of tuning a liner have been studied at GTRI. One of them deals with sliding one perforate[1] over another, thereby changing the perforate porosity and its cross-section, which in turn changes both the perforate reactance and resistance. The second concept utilizes flow passing through a nonlinear perforate. Commonly known as the "bias-flow concept," it was first reported in detail by Dean and Tester[2]. They used positive bias flow implying that the bias flow was in the form of blowing towards the liner face sheet. This concept takes advantage of the role that a nonlinear buried septum plays in determining the overall absorption of a 2DOF liner. Steady airflow through a perforate or orifice has been shown to increase its impedance[3]. The amount of air needed to affect a change in the perforate impedance is dependent on the relative nonlinearity of the perforate, i.e., the more nonlinear, the more impedance change for a given amount of steady airflow. Thus, bias flow through a nonlinear buried septum can be used to change the acoustic properties of a 2DOF liner.

This report investigates how the sound absorption of a 2DOF liner is enhanced with negative bias flow. Such a flow is produced via flow suction through the septum in the direction of the backwall. Bias flow can be produced either by letting flow through the buried septum in either directions: towards the face sheet or away from the face sheet towards the backwall. In either case, the velocity gradient on the face sheet may be affected by the mass injected into or drawn from the boundary layer. Since positive bias flow results by Dean and Tester[2] were found to be quite effective, and little data was available in the open literature on negative or suction bias flow, the present study focused its efforts on the negative bias flow effects. It was also felt that if shown to be successful, it could be used in conjunction with laminar flow control for those applications where a need exists to reduce skin friction over the liner surface.

The normal incidence absorption of the liner was measured in an impedance tube for varying amounts of bias flow. The insertion loss was then measured by placing the liner along the wall of a flow duct. Results for varying degrees of grazing and bias flow are presented.

2.0 Experimental Approach and Facilities

2.1 2DOF Liner Design

Two liners were fabricated, one for normal incidence testing in an impedance tube and another for flow-duct testing. Both liners are described in detail in reference[1]. In reference 1, a septum with a range of porosities was tested. In this study, two septum porosities were used: 2% and 19.5%. The basic geometrical parameters of the liners are summarized below:

Face sheet
h = 0.032 in.
r = 0.03125 in.
σ = 19.5% accounting for honeycomb cell blockage

Buried Septum
h = 0.064 in. [2 sheets, each 0.032 in.-thick]
r_{eq} = 0.01 inches
σ =2.0% and 19.5%

Honeycomb Layers
1st Layer depth, L_1 = 0.5 in.
2nd Layer depth, L_2 = 1.25 in.

Back wall
Sandwiched, 0.5-inch thick honeycomb with one 0.10-inch diameter orifice per cell on each side. This was attached to a partitioned plenum described below.

2.2 Design of Liner Back Wall

It was desirable to design a highly resistive back wall that behaves as a hard surface yet allows flow through the liner. Initial attempts were made in achieving this goal by placing various felt metal materials of high resistance behind the liner similar to the approach adopted by Dean and Tester[2]. For positive bias flow, a high-pressure plenum could be used to overcome the high-pressure drop through the highly resistive felt metal layer. In the case of negative bias flow, overcoming large pressure drops through the felt metal turned out to be a major challenge due to inherent limitations in the low-pressure capabilities of existing vacuum pumps. Using less resistant felt metal material was ruled out as it would absorb considerable sound and its impedance would need to be quantified, thus complicating the assessment of bias-flow in changing the impedance of the overall liner.

Another method of accomplishing this task is to design a hard backwall consisting of honeycomb cells sandwiched between two sheets of metal. A single orifice drilled in the sheet metal would be centered on both sides of each honeycomb cell. This backwall would act as a Helmholtz resonator and would be highly absorbent only at its resonant frequency. At all other frequencies, the design should provide a virtual hard wall while still allowing flow through the liner. A plenum cavity was used behind the backwall to facilitate air suction. To reduce any acoustic cross talk between the individual honeycomb chambers, the partitioned plenum fitted with porous tubings shown in Figures 1c was placed behind the hard wall. The back wall would be positioned behind the liner and mounted to the impedance tube as shown in the schematic in Figure 1a. A detailed view of the positioning of the test liner between the impedance tube and bias flow back wall is shown in Figure 1b. Figure 1c shows the partitioned plenum cavity behind the back wall.

The components used to construct this backwall are shown in Figure 2. The backwall and the partitioned plenum together form a double-Helmholtz resonator system. Since the resonant frequency of this combination is a strong function of the orifice diameter and honeycomb cell and partition plenum volume, a parametric study could be performed to find a suitable geometry to achieve low sound absorption in the frequency range of interest. As an initial guess, the resonant frequency was estimated through calculations presented by Blevin[4] where the back wall and partitioned plenum can be modeled as two unequal, coupled double vented resonators shown in Figure 3. Such a double resonator arrangement has two frequencies of resonance: one is associated with the honeycomb cell volume and the other with the partitioned plenum volume. Figure 4 shows these solutions for a constant partition plenum volume and a varying honeycomb cell volume. The lower resonant frequency associated with the partition plenum is centered approximately at 200 Hz. The resonant frequency associated with the honeycomb cell volume is strongly dependent on the honeycomb depth. It was desirable to minimize the honeycomb depth in order to push the resonant frequencies to regions that were not near the resonance frequencies of the 2DOF liner.

This backwall and partition plenum were placed directly behind the 2DOF liner and each back wall orifice was positioned at the geometric center of each honeycomb cell of the liner to provide each honeycomb with its own suction plenum chamber. Uniform suction was distributed through each of the individual partitioned plenums behind the back wall.

2.3 Normal Incidence Impedance Tube

Normal incident impedance measurements were made in an impedance tube that utilized the *Two Microphone Methodology* of impedance determination[5].

The impedance tube consisted of a steel tube that has an inner diameter of 29 mm (1.14 in). The inner diameter is such that plane wave propagation will persist until a frequency of about 6400 Hz is reached. Above this frequency, higher-order duct modes exist. One end of the tube has an acoustic driver attached, while the other end can be configured to have a liner sandwiched between a flange and the back wall (see Figure 1a). The tube has two flush-mounted microphone ports near the terminating flange in order to facilitate the impedance measurement. These microphones are located at a distance of 2.08 inches and 1.25 inches from the sample face location, respectively. The tube is mounted horizontally on wooden supports.

Suction of air through the liner was obtained by connecting a 1-inch diameter tube to a model no. 6024 EXAIR air amplifier shown in Figure 5. Shop air at 80 psig flows through an ejector, which creates negative pressure within the air amplifier and hence suction through the liner. The impedance tube had an inlet section installed just downstream of its acoustic driver to entrain ambient air (see Figure 1a). The inlet section consisted of a 3-inch long duct section with 8, equi-spaced, 0.1-inch diameter holes.

The liner was sandwiched between the back wall and the flange of the impedance tube. Since the inner diameter of the impedance tube is 1.14 inches, only seven honeycomb cells within the liner were exposed to any normal incident sound waves. Suction was provided to

only one of the partitioned plenums since it contained all of the aforementioned seven honeycomb cells. A Flow-Dyne venturi meter with a throat diameter of 0.25 inches was used to calculate the bias mass flow rate.

2.4 Flow Duct Facility

Insertion loss experiments were conducted in a flow duct facility modified for bias flow implementation. The 2DOF liner was tested under grazing flow conditions in a non-anechoically terminated, rectangular flow-duct. Insertion loss was measured as a function of grazing flow velocities and bias flow Mach numbers. The flow-duct was configured such that sound and flow originated upstream of the liner section placed in the duct. This facility consisted of a high-pressure plenum, a converging duct section, and a constant-area duct section shown in Figure 6. At some distance along the constant area section, a liner housing section was placed. Upstream of this location, acoustic energy was allowed to enter the duct via two ports on the side. The constant area duct section was rectangular (4.69 inches x 2.00 inches). At a temperature of 72°F, a purely plane wave will propagate up until a frequency of 1450 Hz when the 1st higher mode is cut-on.

Figure 7 shows a photographic view of the experimental set-up for the insertion loss tests. Acoustic measurements were made outside of the flow-duct on a radius of 2 feet from the center of the duct exit plane at polar angles of 30, 60, and 90-degrees. These measurements were made as a function of grazing flow, first with a rigid wall and then with the liner installed on a portion of one side of the duct. The difference between the rigid wall and the lined results provided the insertion loss. A sweep signal was supplied to the acoustic drivers and the microphone data was sampled with 64 averages over a frequency range of 0 - 6400 Hz with a bandwidth of 4 Hz. All measured data is presented in 1/3 octave bands. This provided a preliminary assessment of the ability of the liner to change its absorption characteristics and, thus, its wall impedance.

3.0 Instrumentation, Data Acquisition and Reduction

Acoustic Driver

Sound was generated in the impedance tube with a JBL Model 2446J acoustic driver in conjunction with a Carvin 1500 amplifier and a HP 33120A digital function generator. Broadband overall sound pressure levels of 150 dB were achieved. Sound was generated in the flow-duct with two Electro Voice Model 2012 acoustic drivers.

Microphones

For the impedance tests, Bruel & Kjaer (B&K), phase-matched _-inch, type 4187 microphones were used in conjunction with B&K type 2633 pre-amplifiers. The B&K microphones and pre-amplifiers were powered by a B&K 2804 power supply. Output from this power supply was fed directly into an FFT analyzer. The farfield microphones for the insertion loss tests were _-inch type 4133 B&K microphones. These microphones were calibrated daily for amplitude using a B&K 4231 pistonphone which produces a 1 kHz tone at 114 dB in order to provide an absolute baseline sound pressure level.

Signal Processing

The microphone signals were fed into an HP 3667A Multi-Channel Signal Analyzer for FFT analysis. The analyzer was operated from a Windows 95 platform on a Pentium 200 MHz computer. Implementation of the Two-Microphone impedance technique requires that one microphone be the reference signal for the other microphone in order for the cross-correlation of the two signals to be performed. The FFT analysis was performed in a frequency range of 0–6400 Hz with a bandwidth of 4 Hz. A Hanning window with 50% overlap was used for all analyses. 64 averages were used when sampling the microphone signals. In the impedance tube tests, the signal from microphone A (furthest from sample face) was used as the reference for the cross-correlation analysis.

4.0 Results

4.1 Normal Incidence Impedance of Bias Flow Back Wall

4.1.1 Controlling Back Wall Resonant Frequency

The design of the backwall was to resemble a Helmholtz resonator. This meant that varying the backwall orifice diameter, honeycomb cell depth, and partitioned plenum volume, would control the resonant frequency. The goal was to design these parameters such that the back wall and partitioned plenum mimicked a hard wall. This would be approximately the case at frequencies other than the resonant frequencies of the resonator. Thus, a successful backwall for the bias flow liner configuration should be comparable in performance to a rigid back wall for the conventional liner configuration.

Figure 8 shows the normal incidence absorption coefficient of the 2DOF liner with a truly rigid backwall and with the bias flow backwall configuration described in the previous section. The backwall honeycomb depth was 0.5 inches and the partitioned plenum volume was 109.25 in^2. The liner in both cases was exposed to a broadband acoustic signal and the buried septum had a porosity of 19.5%. Except for the region between 1800 Hz and 2800 Hz where the resonance of the backwall is dominant, there is reasonable agreement between the bias flow backwall and the rigid backwall configurations. This is a significant result because it shows that a pseudo-rigid backwall can be created while still providing enough open area for steady airflow. This configuration with the geometrical dimensions provided dimensions provided here was used for the main experiments described here.

In order to arrive at the result shown in Figure 8, the choice of the appropriate honeycomb depth and partitioned plenum had to be made. This involved performing a series of parametric studies. The backwall alone was mounted to the end of the impedance tube and a series of experiments were first performed to determine the normal incident impedance without any bias flow. Two honeycomb samples of nominal depths of 0.5 and 1.25 inches, respectively, were tested while maintaining the plenum partition volume and orifice size constant. The absorption coefficient using the broadband input signal is shown in Figure 9. High absorption at two Helmholtz resonance frequencies and their vicinity are evident. It is found that varying the honeycomb cell volume had a strong effect on the value of these resonant frequencies. No change was noticed for the first resonant frequency of 200 Hz since the partitioned plenum volume is constant at 109.25 in^3 and this frequency is a function of

the volume of the partitioned plenum volume. By decreasing the depth of the honeycomb and hence its volume, the second resonant frequency is shifted from 1400 Hz to 2200 Hz as seen in Figure 9.

To obtain a large region of low absorption in between the two resonant frequencies, it is not only desirable to force the secondary resonant frequencies to high values but also to force the first frequency close to zero. This can be accomplished by increasing the volume of the partitioned plenum. The effect of increasing the partitioned volume while keeping the honeycomb cell volume constant is shown in Figure 10. As the partitioned volume was increased from 24.25 in^2 to 291.5 in^2, the first resonant frequency decreased from 400 Hz to 50 Hz. It was thus necessary to decrease the depth of the honeycomb cell and increase the partitioned plenum volume in order to spread out the two peak frequencies. It is also observed that the absorption coefficient is about 0.1 for a frequency range of 2.5 kHz to 6kHz. All remaining tests were performed with a bias flow back wall honeycomb depth of 0.5 inches and a partitioned volume of 109.25 in^3.

4.1.2 Effect of Negative Bias Flow on Back Wall Plenum

In reality, the backwall when mounted above the partition plenum can be treated as a "stand alone liner" designed to absorb sound primarily at the appropriate resonant frequencies as discussed above. Since air is being drawn through the orifices of the backwall into the plenum, it was felt that examining the effect of bias flow though this backwall plus partitioned plenum was critical prior to testing the effect of bias flow on the liner performance. Ideally, if there is a negligible effect of bias flow on the impedance of the back wall, the back wall will appear rigid to incident sound. The absorption coefficient of the backwall alone with varying amounts of bias flow are shown in Figure 11. The absorption coefficient increases at frequencies away from the peak absorption frequency. This effect is more pronounced at the frequencies lower than the peak absorption frequency. Thus, the backwall is behaving less like a hard surface for increasing bias flow at lower frequencies up to 2000 Hz.

More insight into the effect of bias flow on the backwall absorption can be discerned from examining the normalized resistance and reactance, which are the real and imaginary components of the normalized impedance, respectively. The absorption coefficient can be calculated from the resistance and reactance using the well known expression for normal incidence plane wave transmission theory shown in equation 1:

$$\alpha = \frac{4\frac{R}{\rho c}}{\left[1+\frac{R}{\rho c}\right]^2 + \frac{\chi}{\rho c}^2} \qquad (1)$$

From this expression it is seen that perfect absorption (α =1) is achieved if the normalized resistance is unity and the normalized reactance is zero. For a typical resonant-type liner, this condition is referred to as liner resonance. Anti-resonance occurs when the normalized

reactance is zero and the corresponding normalized resistance is very large (>>1). The zero reactance is preceded by a very large positive reactance and followed by a very large negative reactance. In general, however, if either the normalized resistance is large compared to unity or the normalized reactance is large compared to zero, the absorption coefficient is small (see equation 1).

Figure 12 and 13 show the normalized resistance and reactance of the bias flow back wall configuration for various amounts of bias flow. Note the anti-resonance frequency is approximately 1600 Hz for the case without bias flow. Also above 3000 Hz, the reactance is large compared to zero which leads to low absorption (see Figure 11). As bias flow is introduced and increased, the normalized resistance at the anti-resonance frequency is reduced while away from anti-resonance the resistance is increased. This is more prominent below 1600 Hz. Bias flow appears to "smooth" the normalized reactance in the vicinity of the anti-resonance frequency, as shown in Figure 13. Indeed at frequencies below 1600 Hz, the normalized reactance almost becomes constant when largest amount of bias flow is introduced. Reactance is also reduced somewhat above 4500 Hz. The bias flow appears to damp the anti-resonance of the liner as evidenced by the lowered reactance near the anti-resonance frequency. This leads to more sound absorption as shown in Figure 11 where bias flow increases the absorption coefficient in the same frequency region as the reduction in normalized reactance. It appears that the introduction of bias flow through the back wall increases the absorption potential of the backwall at lower frequencies. At frequencies higher than about 3 kHz where low absorption was obtained, this backwall arrangement can be assumed to be a hardwall. This result, while not helpful for the purposes of maintaining a rigid back wall, forecasts the positive results to be gained by bias flow passing through the 2DOF liner. These effects must be kept in mind while interpreting the effect of the bias flow on the overall liner.

4.2 Improved Liner Performance with Negative Bias Flow

4.2.1 Normal Incidence Impedance

Normal incidence acoustic measurements were made for a range of negative bias flow rates with the bias flow back wall and partitioned plenum placed behind the 2DOF liner with a buried septum porosity of 2% (see Figure 1b). Figures 14-16 show the corresponding absorption coefficient, normalized resistance, and normalized reactance, respectively. The Mach number of the flow through the buried septum orifices are shown along with the mass flow rates.

It is seen that as the bias flow Mach number is increased, the absorption coefficient also increases. In fact, as the septum Mach number approaches a value of 0.128, the absorption coefficient approaches unity at all frequencies up to 4 kHz as shown in Figure 14. Comparing the data of Figure 11, clearly this broadband absorption is not just the effect of flow though the back wall. It appears to be that due to modifications of the septum impedance. Note that bias flow tends to drive the normalized resistance towards unity. This is seen in Figure 15 above and below 2200 Hz. Furthermore, the bias flow drives the normalized reactance towards zero as seen in Figure 16. This trend is similar to that shown in Figure 12 and 13 where the backwall configuration exhibited a reduction in reactance. From equation 1, it is evident that this behavior will result in high absorption.

It is important to point out that the control of the buried septum impedance and hence the absorption of the entire 2DOF liner is predicated on the nonlinear behavior of the septum. This can be shown by introducing bias flow through the 2DOF liner and setting the porosity of the septum to 19.5%. This configuration results in a lower orifice Mach number in the septum and hence a more linear behavior. Figure 17 shows the absorption coefficient for this configuration. Bias flow was found to have only marginal effects at frequencies higher than 800 Hz. At lower frequencies, the absorption coefficient increased, but it may be an effect of the changes introduced by the bias flow back wall. Note that the mass flow rate through the 2% and 19.5% porosity septa were comparable, but the Mach numbers through the septa was almost an order of magnitude higher for the smaller porosity.

4.2.2 Insertion Loss Results

Insertion loss was measured in the flow-duct using a 2DOF liner similar to that used for impedance testing, mounted in the flow duct facility in the manner shown in Figure 6. Measurements were made as a function of grazing flow velocity and bias flow rate. Due to the limitations in suction capability of the test facility, a maximum septum Mach number of approximately 0.15 could be obtained. A frequency sweep was introduced upstream of the liner via acoustic drivers. Note that this Mach number is much smaller than that obtained in the impedance tube tests. This is because all flow was drawn though the impedance tube cross-section whereas in the 2DOF liner tests, the same overall flow was drawn through the complete liner face sheet.

Figures 18-20 show the sound pressure levels measured at microphones located at polar angles of 30°, 60°, and 90° with respect to the flow direction. The sound pressure levels with a hardwall in place are also shown for comparison. It is seen that as the bias flow Mach number is increased, the farfield noise levels decrease at each of the microphone locations. With respect to the hard wall, the sound pressure levels have decreased at all frequencies up to almost 4.8 kHz. Clearly, the bias flow is reducing the sound pressure levels measured outside of the flow duct at frequencies below 2000 Hz and above 3000 Hz. This is consistent with the impedance tube results, however, the absorption does not appear to be as broadband as seen in the impedance tube tests. One reason for this is that the sound is not normally incident on the liner, thus the amount of acoustic energy exposed to the liner is reduced.

Figure 21 shows the insertion loss of the liner installed in the flow duct for no grazing flow and for increasing negative bias flow. Since similar trends are observed for data measured at the 30°, 60°, and 90° microphones, only 30° insertion loss data is presented here. The peak absorption at 1400 Hz is attributed to primary resonance frequency of the 2DOF liner. With the addition of bias flow, the peak absorption is increased by about 10 dB. Below this frequency, the insertion loss is increased almost 16 dB. Increased absorption above 3000 Hz is also observed.

The insertion loss for grazing flow Mach numbers of 0.10, 0.15, and 0.20 are shown in Figures 22, 23, and 24, respectively. It is evident that the bias flow effectiveness at and below the peak absorption frequency is diminished. Bias flow is marginally effective at frequencies above 3000 Hz.

The decreased effectiveness of bias flow on liner absorption with increasing grazing flow could possibly be attributed to a reduction in the boundary layer near the liner. The suction occurring at the liner face will reduce the boundary layer thickness produced by the grazing flow. It has been established[6] that the velocity gradient near a wall typical of that produced in these tests tends to refract sound away from the wall and towards the duct exit when the sound and mean flow are traveling in the same direction. Thus, it is possible that negative bias flow will contribute to a greater refraction of acoustic energy away from the liner when the sound and mean flow are travelling in the same direction. This effect is expected to be reversed for the case when sound and the mean flow are travelling in opposite directions, as is the case of jet engine inlets. Further study is needed to quantify this effect and apply negative bias flow to a liner installed in an inlet-type duct.

5.0 Concluding Comments

The effects of negative bias flow on a 2DOF liner have been shown in a normal incidence impedance tube and a flow-duct with mean grazing flow. A summary of the findings are listed below:

1) A back wall that can be porous enough to flow proper amounts of steady air, yet hard enough to act as a rigid wall at certain frequencies can be made by making use of Helmholtz resonators.

2) Negative bias flow will affect the back wall apparatus used for suction by increasing the absorption properties of the back wall.

3) Broadband (between 500 and 4000 Hz) normal incidence absorption was achieved with septum bias flow Mach numbers of 0.128 to 0.311.

4) Negative bias flow increased absorption of a 2DOF liner installed in a flow-duct with zero mean grazing flow. Insertion loss was increased 10 to 16 dB in the 500 to 1400 Hz range.

5) The effect of negative bias flow on insertion loss with a mean grazing flow present in the flow-duct was diminished compared to zero grazing flow.

It is evident from the zero grazing flow absorption measurements (both impedance tube and flow-duct), that negative bias flow enhances the sound absorption of a 2DOF liner. This has implications for noise-control in many situations where grazing flow in not present, such as anechoic chambers and auditoria walls. The reduced effectiveness of negative bias flow in the presence of grazing flow is quite likely related to the boundary layer modification brought about by the suction. Further studies of the effect of negative bias flow in an inlet environment are needed to realize its true potential.

6.0 References

1. Ahuja. K. K. and Gaeta, R. J. *Sliding Perforate Report*

2) Dean, P. D. and Tester, B.J. *Duct Wall Impedance Control as an Advanced Concept for Acoustic Transmission* , NASA Contractor Rept. CR-134998, Nov., 1975.

3) Ingard, U. and Ising, H. *Acoustic Nonlinearity of an Orifice* Journal of the Acoustical Society of America, Vol. 42, No. 1, 1967.

4) Blevins, R.D. *Formulas for Natural Frequency and Mode Shape* Published by Robert E. Krieger Publishing Co., Inc., 1984.

5) Chung, J. Y. and Blaser, D. A. *Transfer Function Method of Measuring In-Duct Acoustic Properties: I. Theory* Journal of the Acoustical Society of America, Volume 68, No. 3, Sept., 1980.

6) Nayfeh, A., Kaiser, J. and Telionis, D. *Acoustics of Aircraft Engine-Duct Systems* AIAA Journal, Vol. 13, No. 2, Feb. 1975.

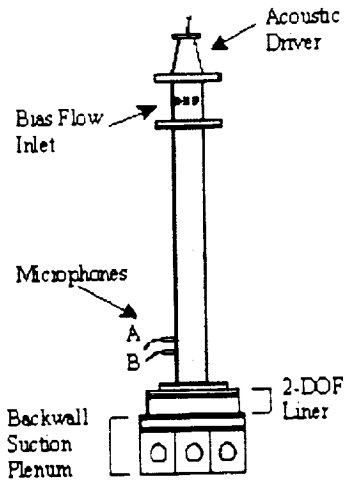

Figure 1a. Impedance tube modified for bias flow tests.

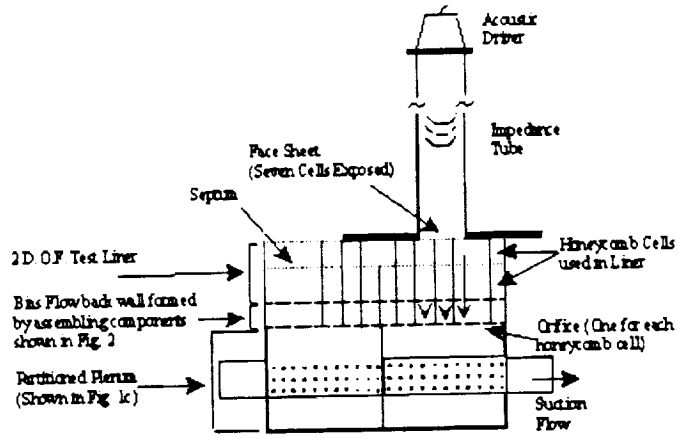

Figure 1b. Geometry of the test liner with negative bias flow.

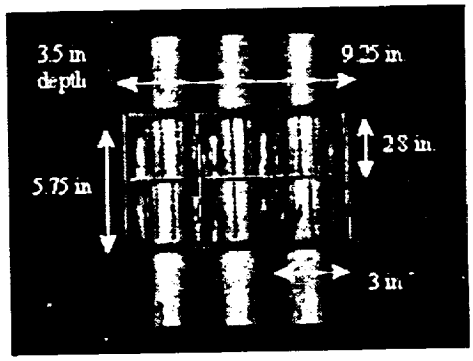

Figure 1c. Partitioned plenum (only one of the six partitions was used to provide suction through impedance tube).

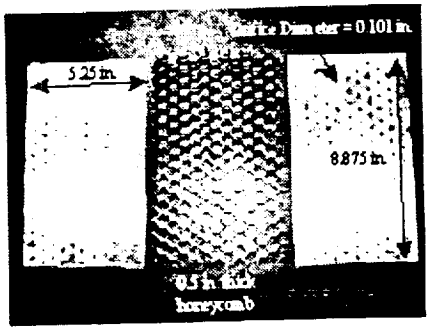

Figure 2. Bias flow back wall components

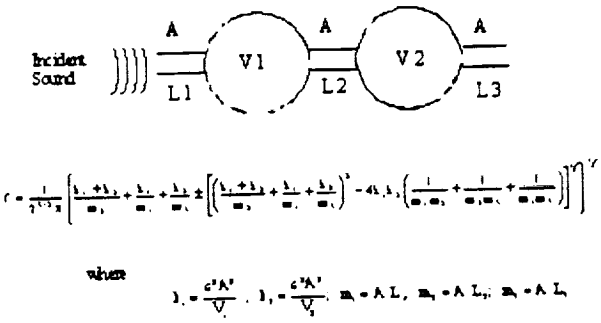

Figure 3. Two unequal, coupled-vented resonator prediction (Blevins[5])

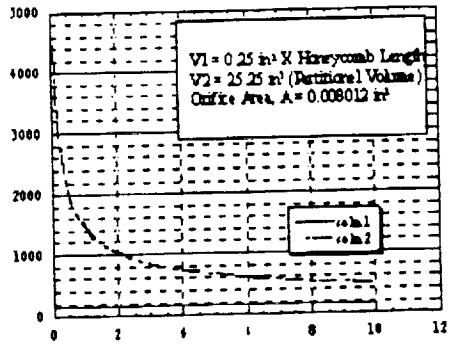

Figure 4. Dependence of resonant frequency on honeycomb depth.

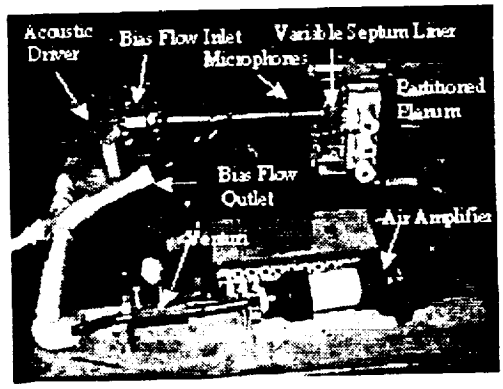

Figure 5. Normal incident impedance test with bias flow.

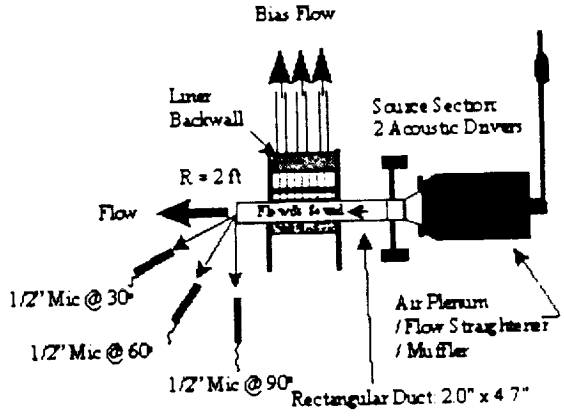

Figure 6. Insertion loss tests in flow duct facility

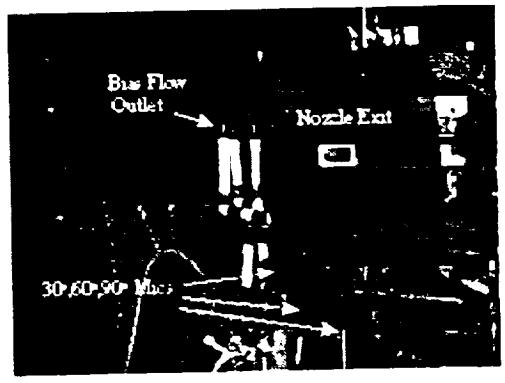

Figure 7. Experimental set-up for insertion loss tests

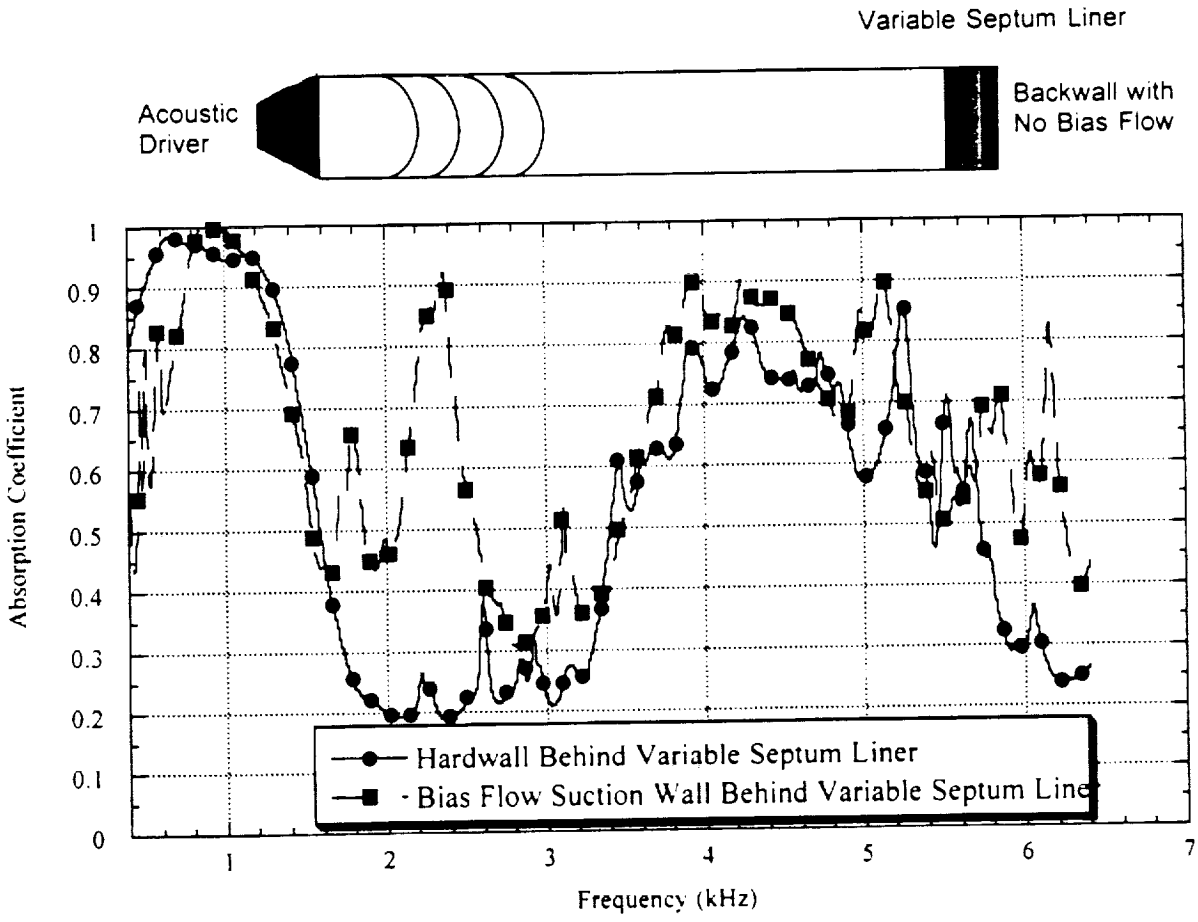

Figure 8. Effect of absorption coefficient on the liner back wall for a broadband input signal [64 avgs.; Δf = 4 Hz] Test98-25 . 26a

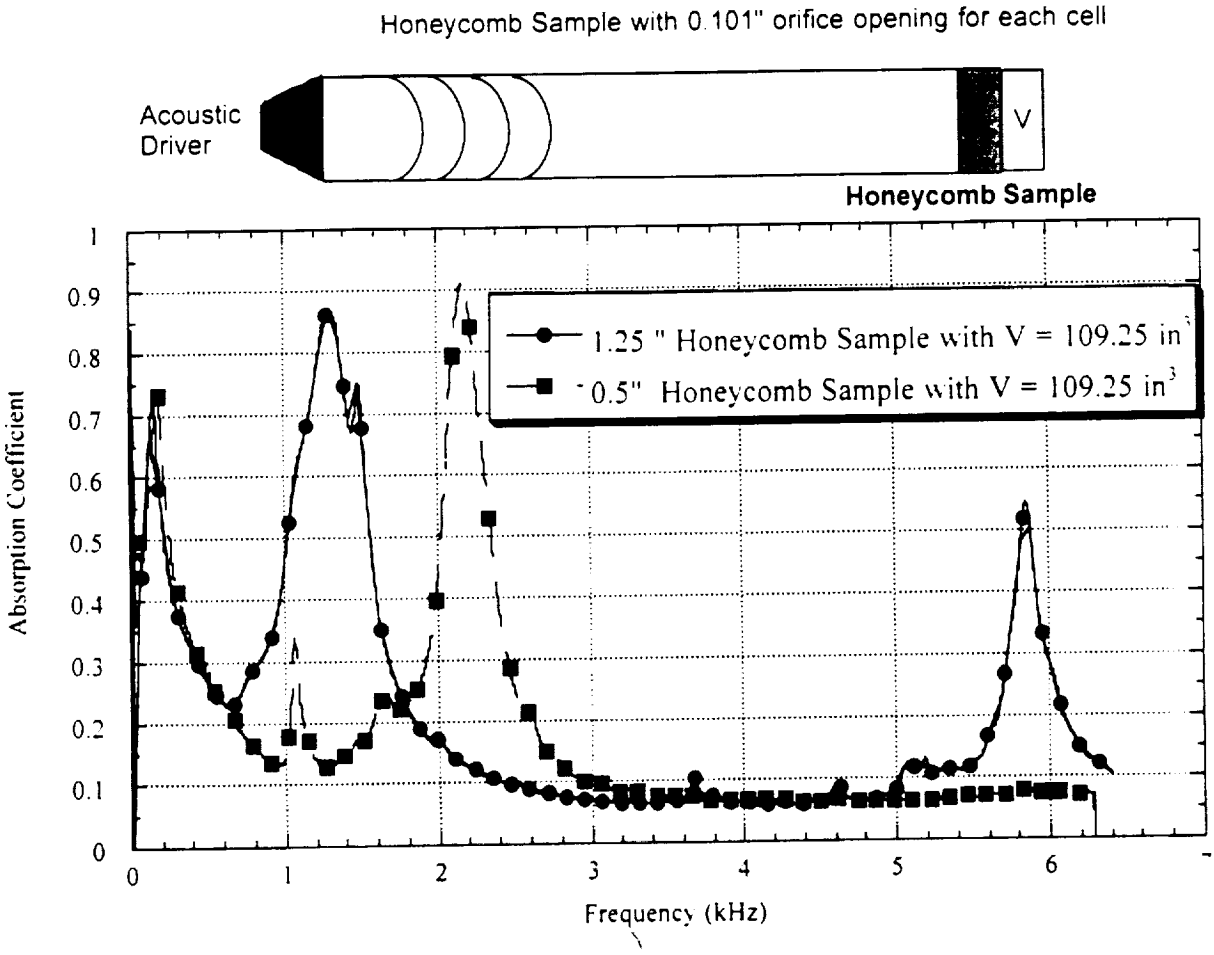

Figure 9. Effect of liner resonant frequency with same backing partion; absorption coefficient for a broadband input signal [64 avgs.; Δf = 4 Hz] Test98-14-17

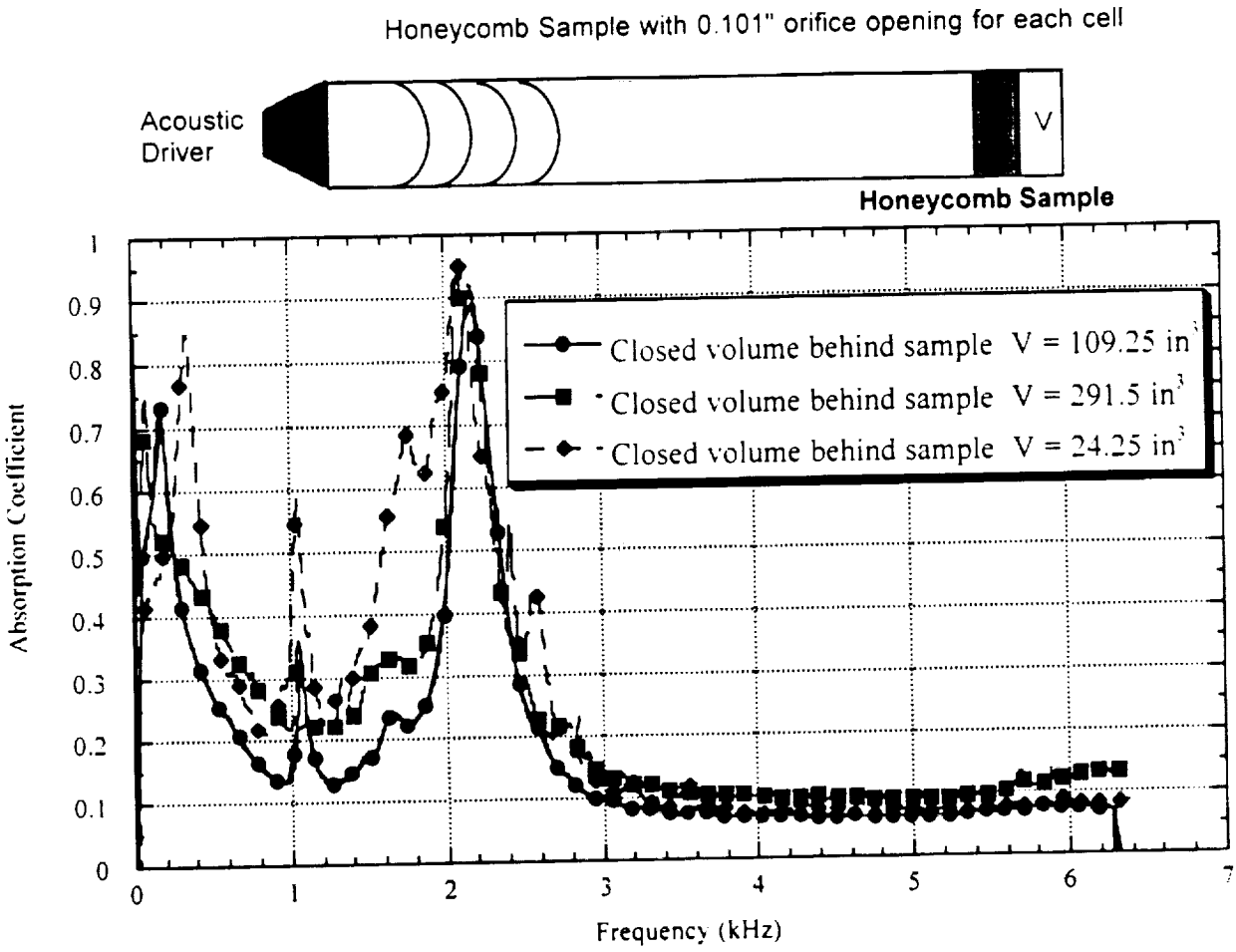

Figure 10. Effect of backing partion volume on absorption coefficient for a broadband input signal [64 avgs.; Δf = 4 Hz] Test98-17,18,19

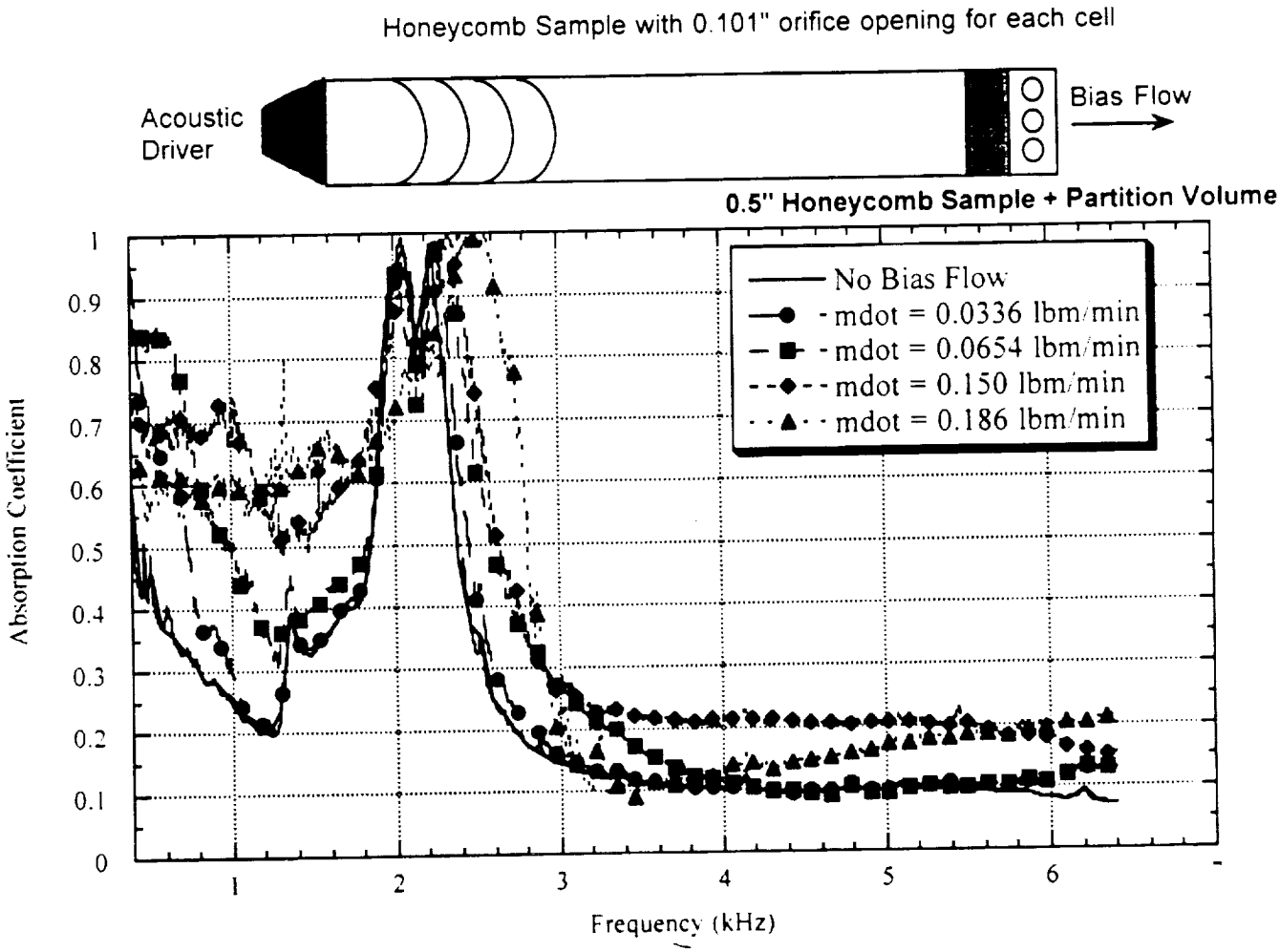

Figure 11. Effect of bias flow on back wall; Absorption Coefficient for a broadband input signal [64 avgs.; Δf = 4 Hz] Test98-23b,c,24a,b,e

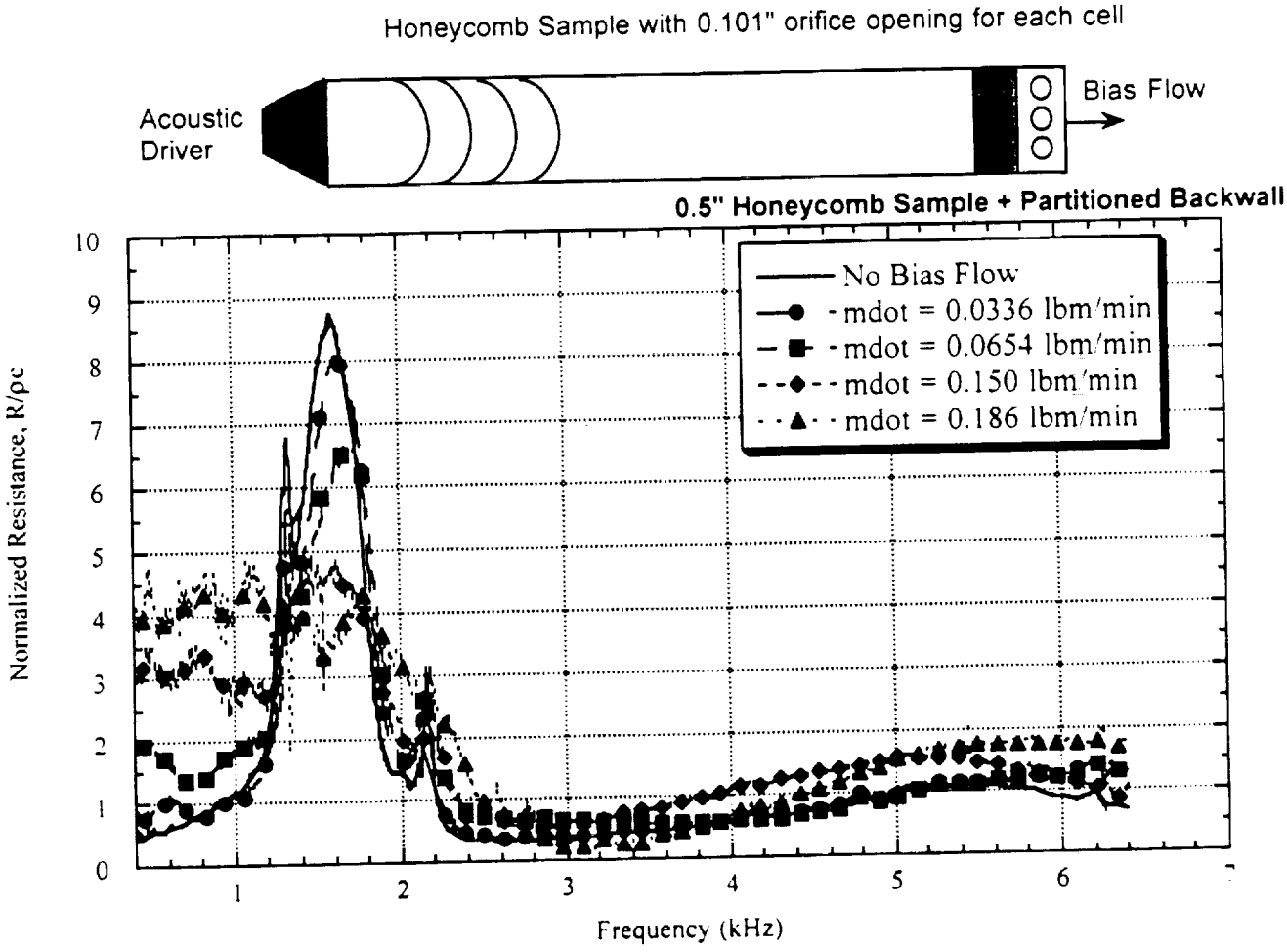

Figure 12. Effect of bias flow on back wall; Normalized Resistance for a broadband input signal [64 avgs.; Δf = 4 Hz] Test98-23b,c,24a,b,e

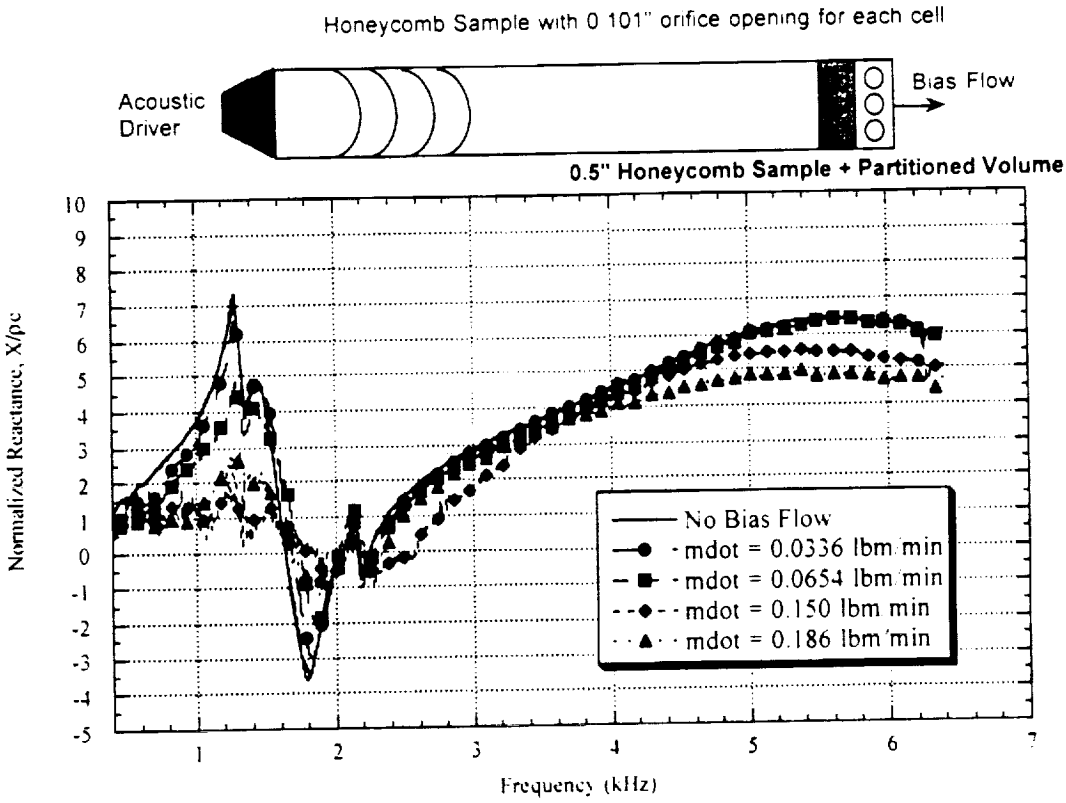

Figure 13. Effect of bias flow on back wall: Normalized Reactance for a broadband input signal [64 avgs.; Δf = 4 Hz] Test98-23b,c,24a,b,e

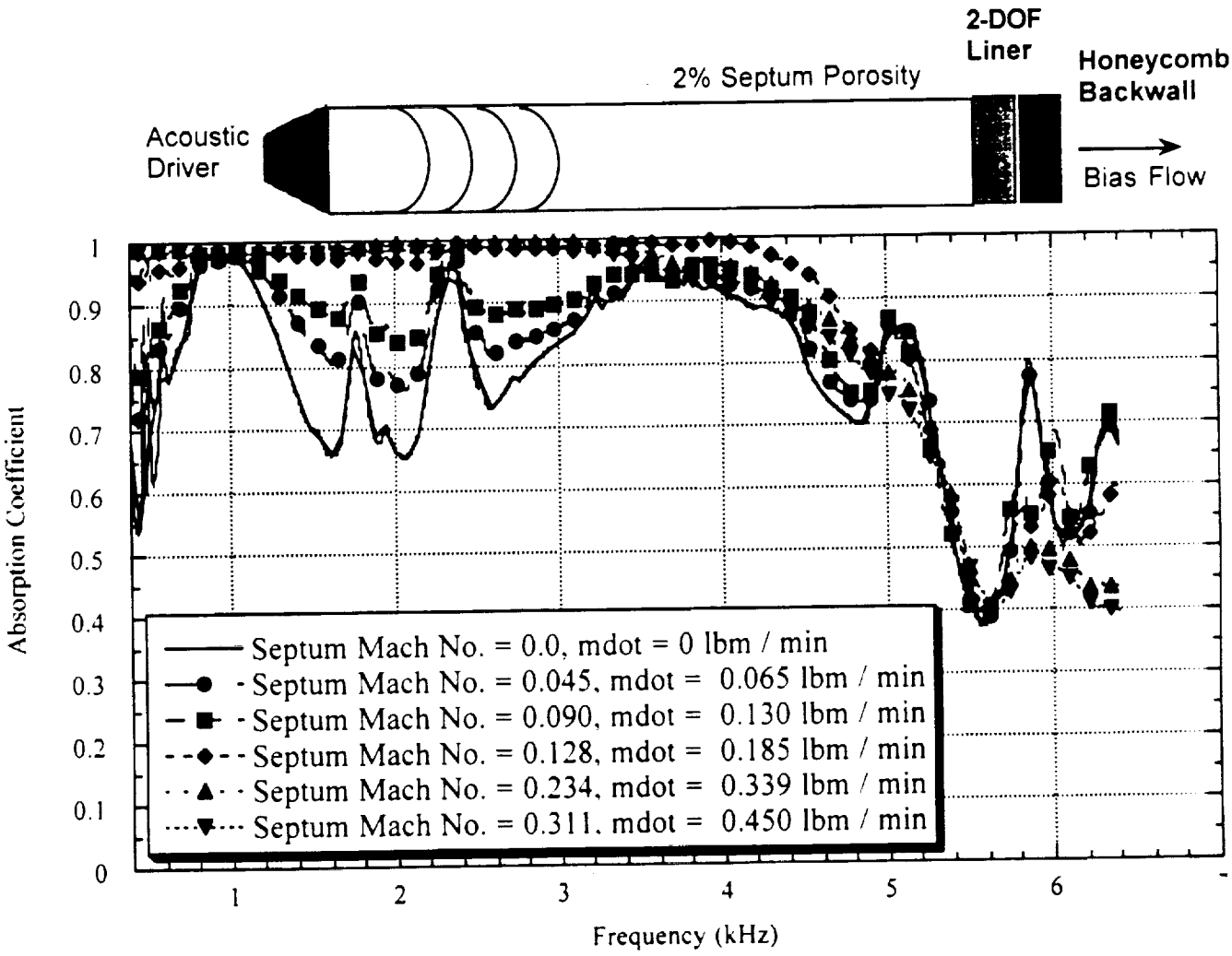

Figure 14. Effect of bias flow on 2DOF liner; Absorption Coefficient for a broadband input signal [64 avgs.; Δf = 4 Hz] Test98-27a,f,l,h,i,j

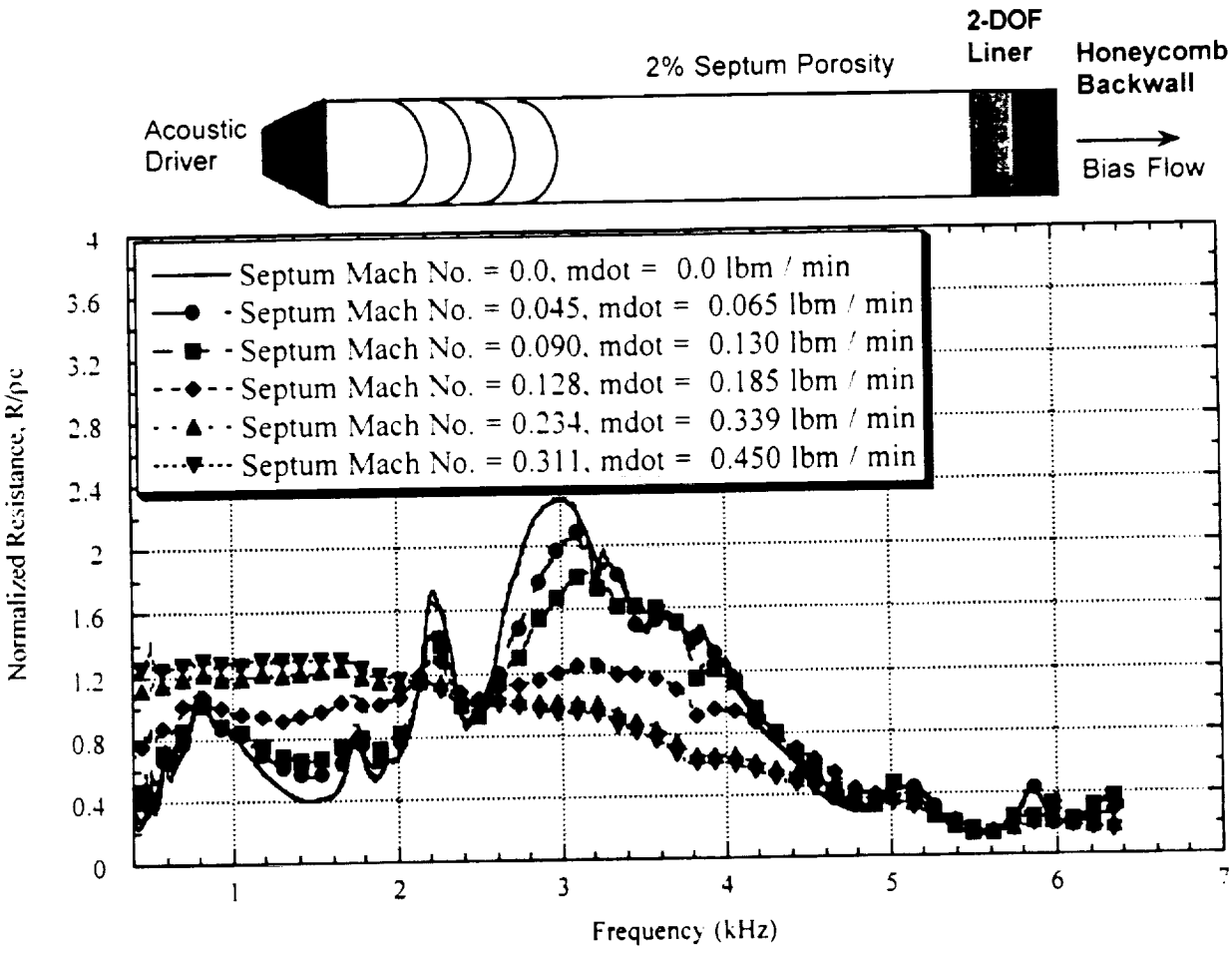

Figure 15. Effect of bias flow on 2DOF liner; Normalized Reactance for a broadband input signal [64 avgs.; Δf = 4 Hz] Test98-27a,f,l,h,i,j

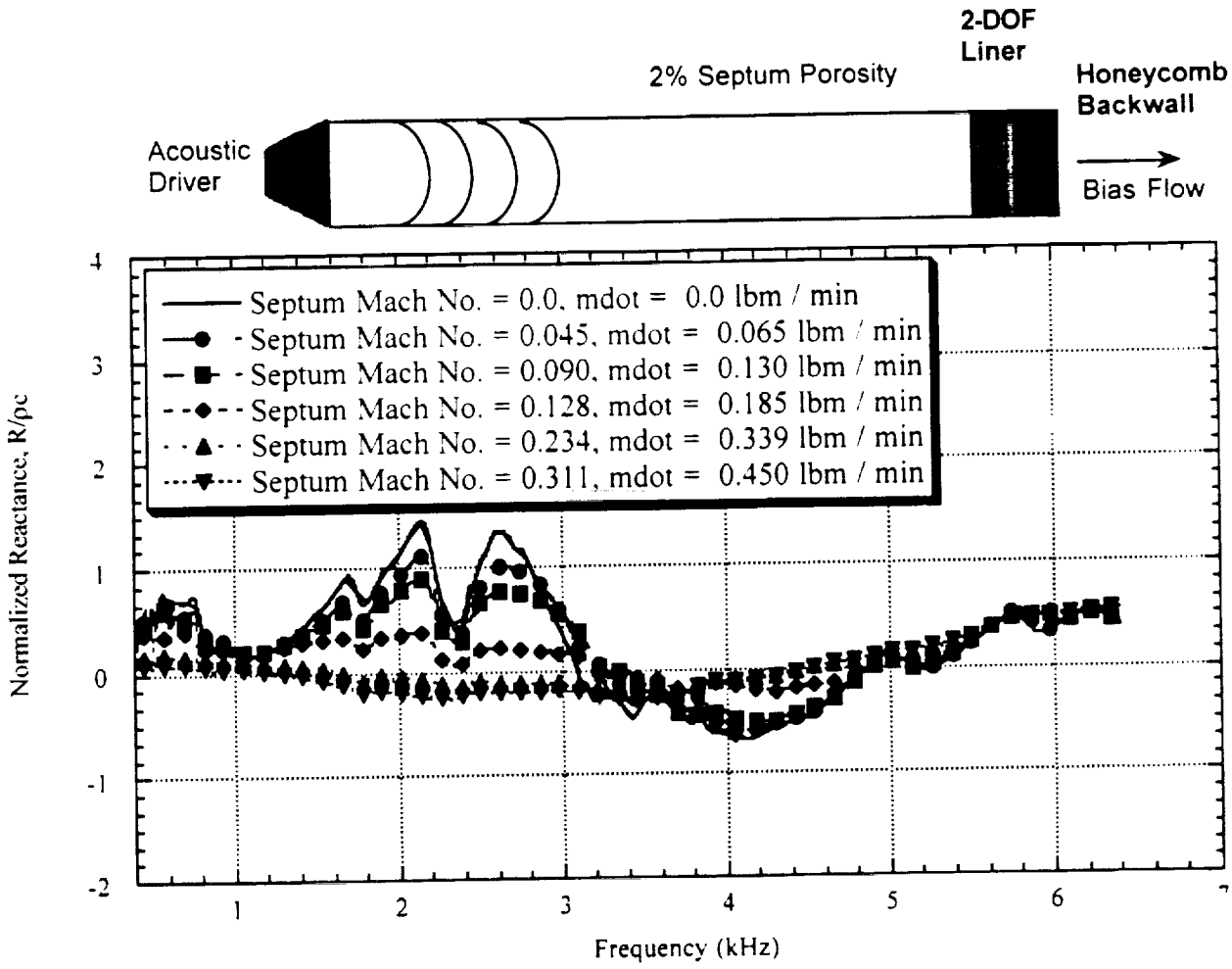

Figure 16. Effect of bias flow on 2DOF liner; Reactance for a broadband input signal [64 avgs.; Δf = 4 Hz] Test98-27a,f,l,h,i,j

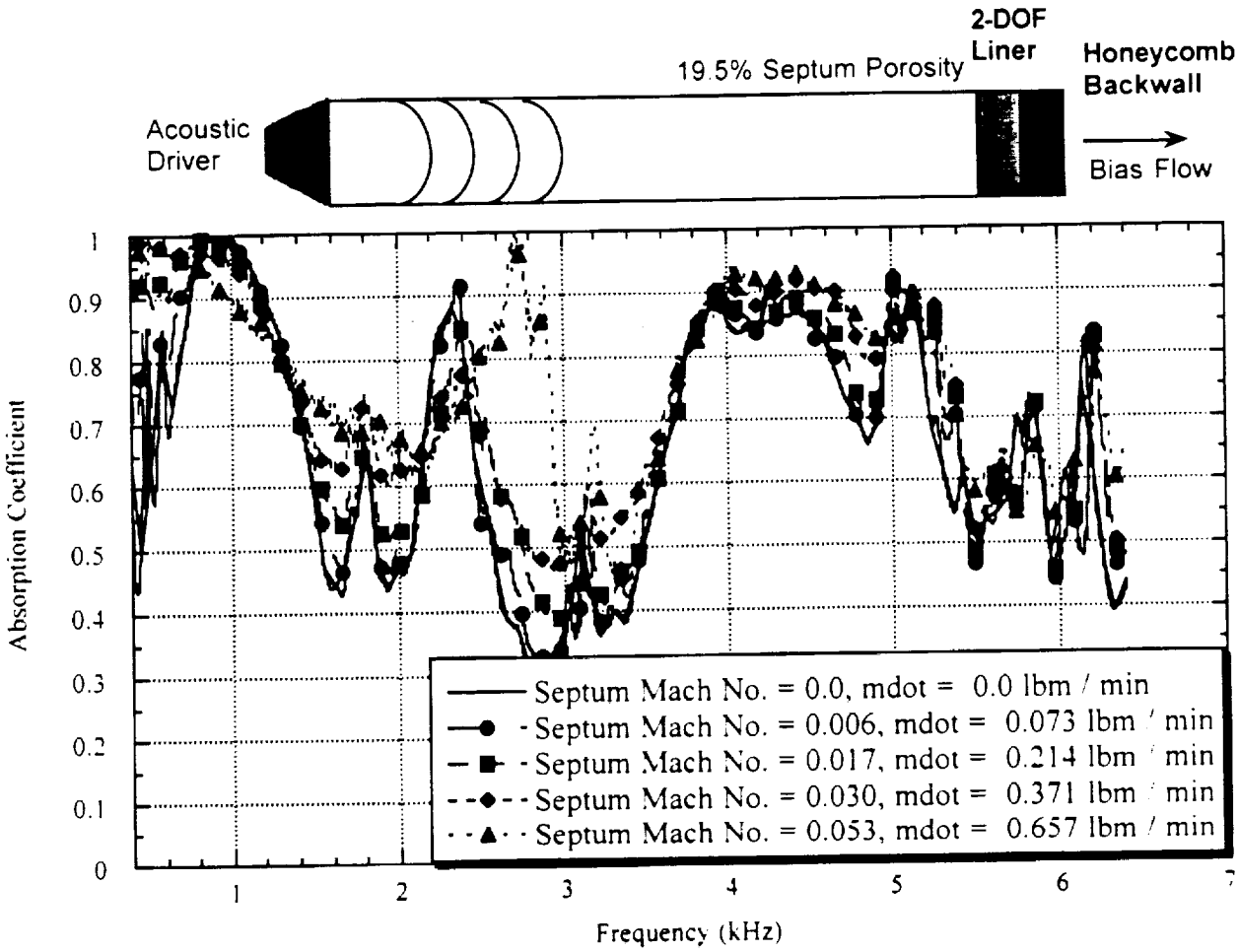

Figure 17. Effect of bias flow on a 2DOF liner with high porosity septum; Absorption Coefficient for a broadband input signal [64 avgs.; Δf = 4 Hz] Test98-26a,d,g,j,l

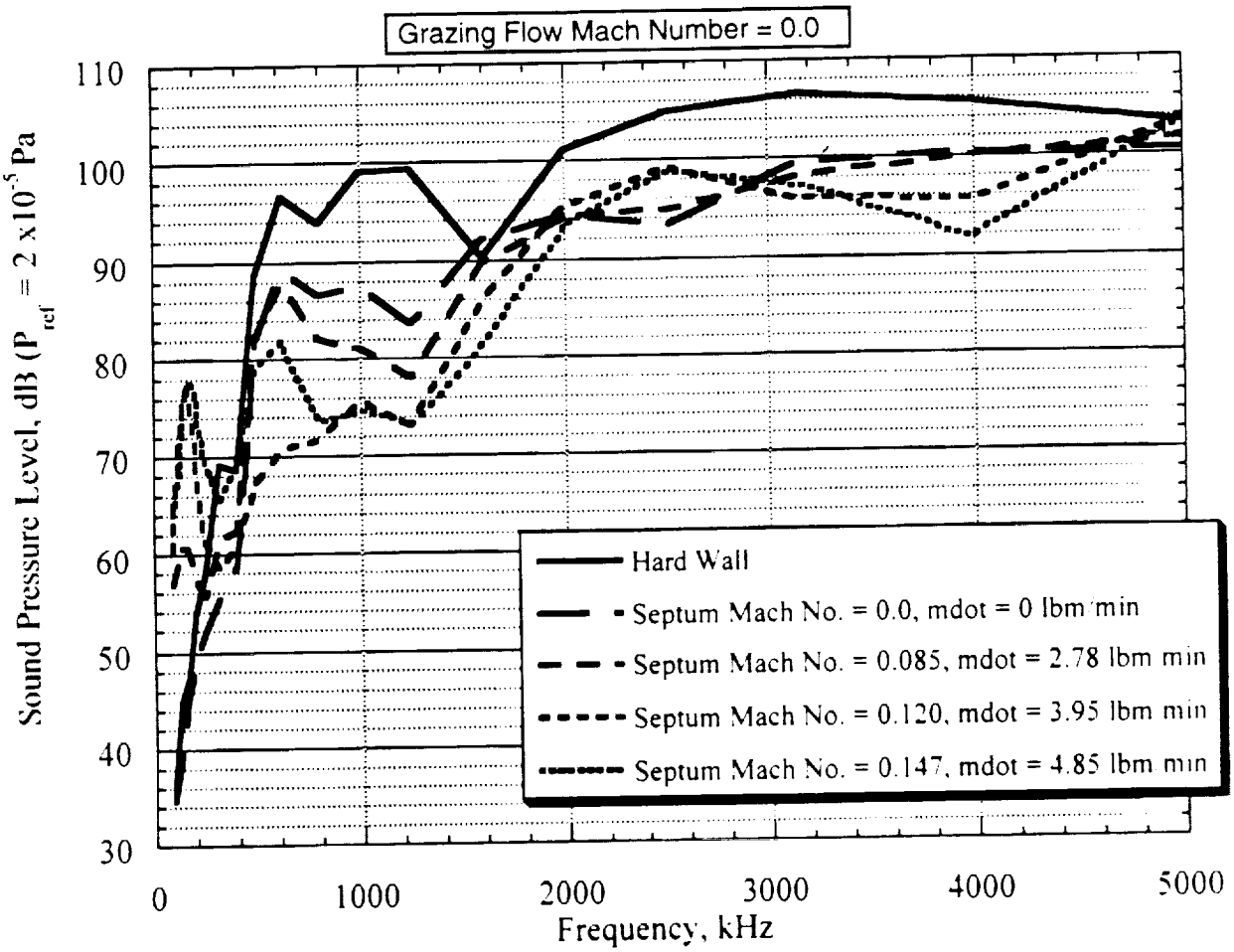

Figure 18. Effect of Negative Bias Flow on SPL at 30° Farfield Mic (500 Hz - 6400 Hz Sweep Input, 64 Avgs, 1/3 Octave Band) Test bs3

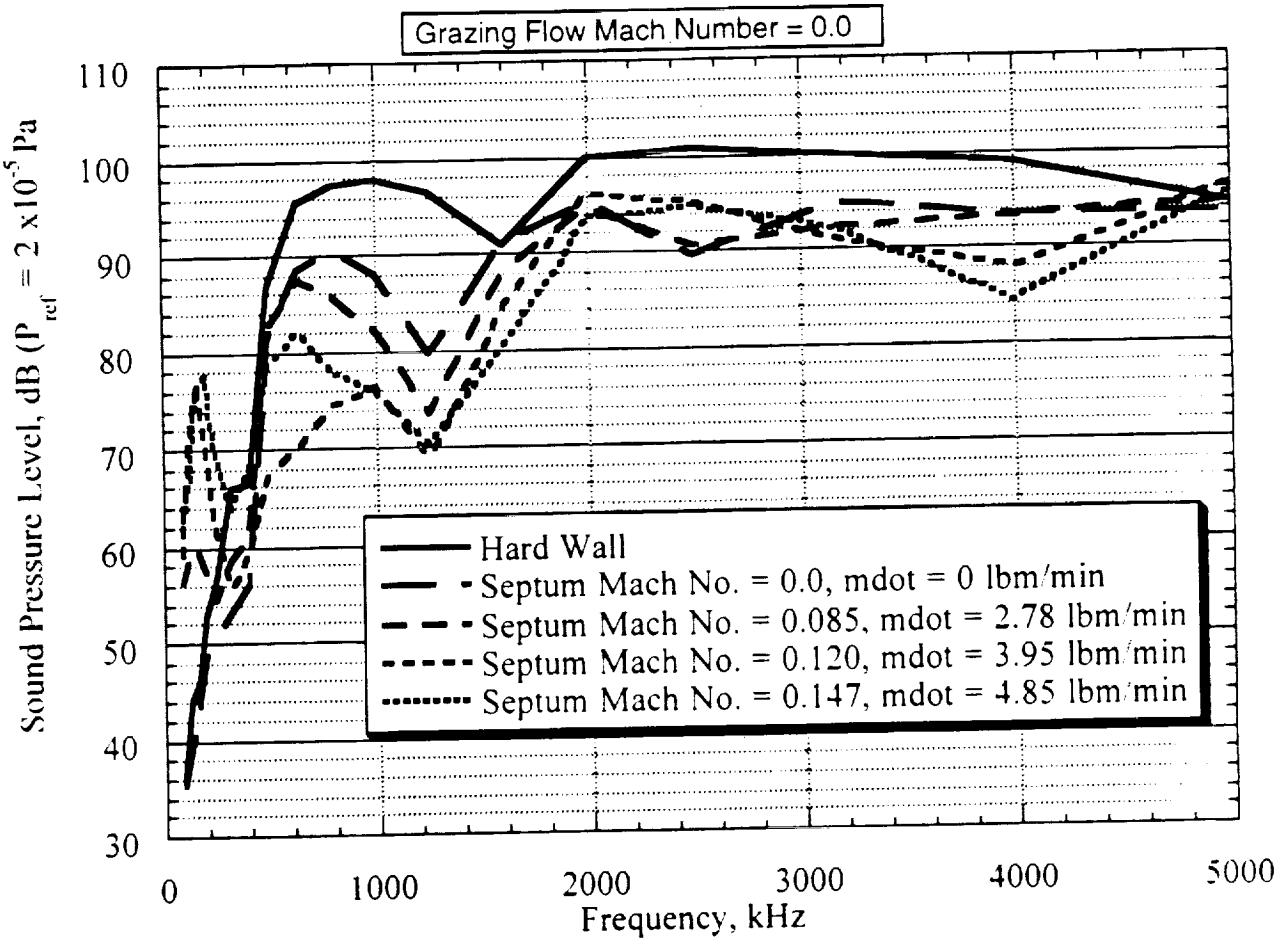

Figure 19. Effect of Negative Bias Flow on SPL at 60° Farfield Mic (500 Hz - 6400 Hz Sweep Input, 64 Avgs, 1/3 Octave Band) Test bs3

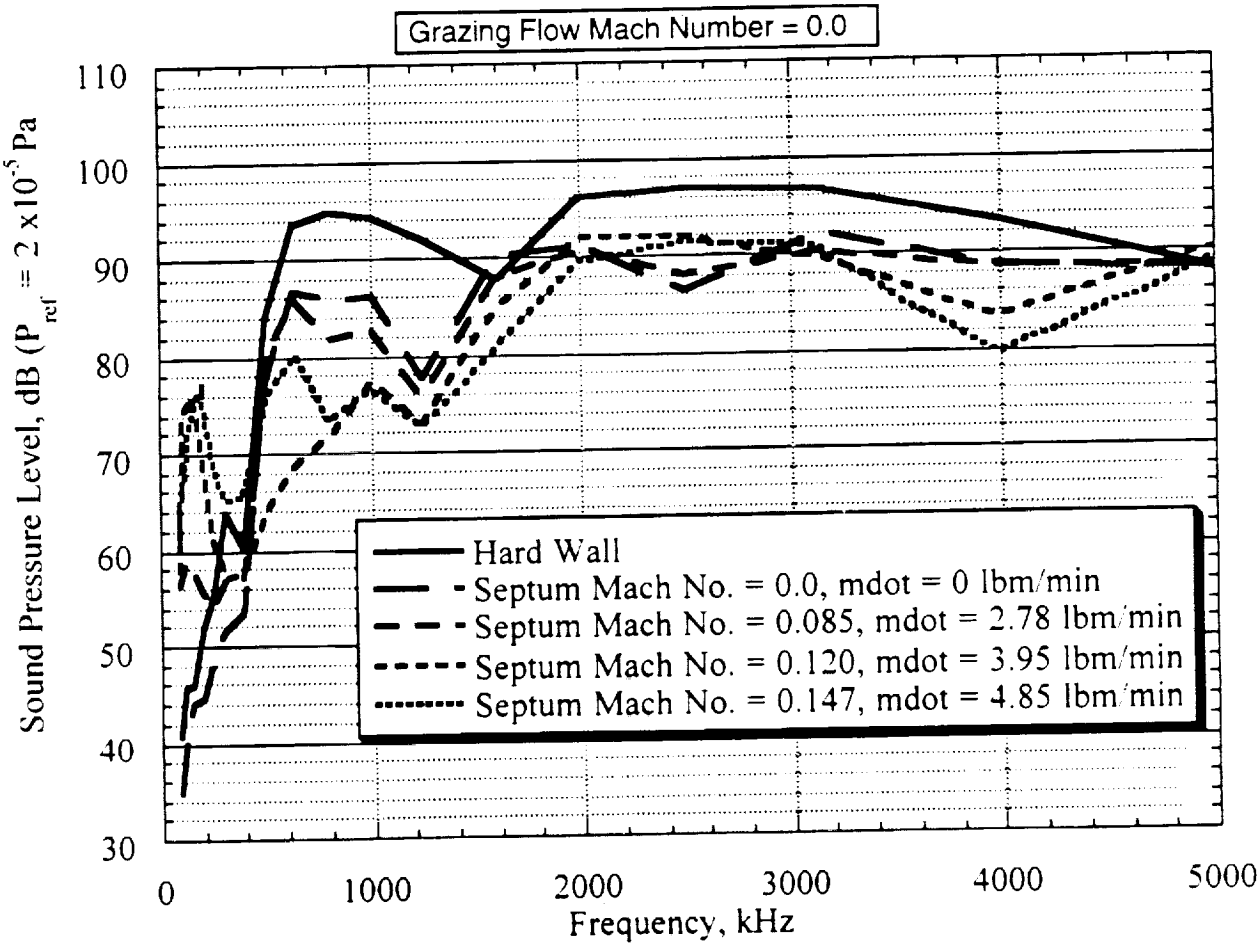

Figure 20. Effect of Negative Bias Flow on SPL at 90° Farfield Mic (500 Hz - 6400 Hz Sweep Input, 64 Avgs, 1/3 Octave Band) Test bs3

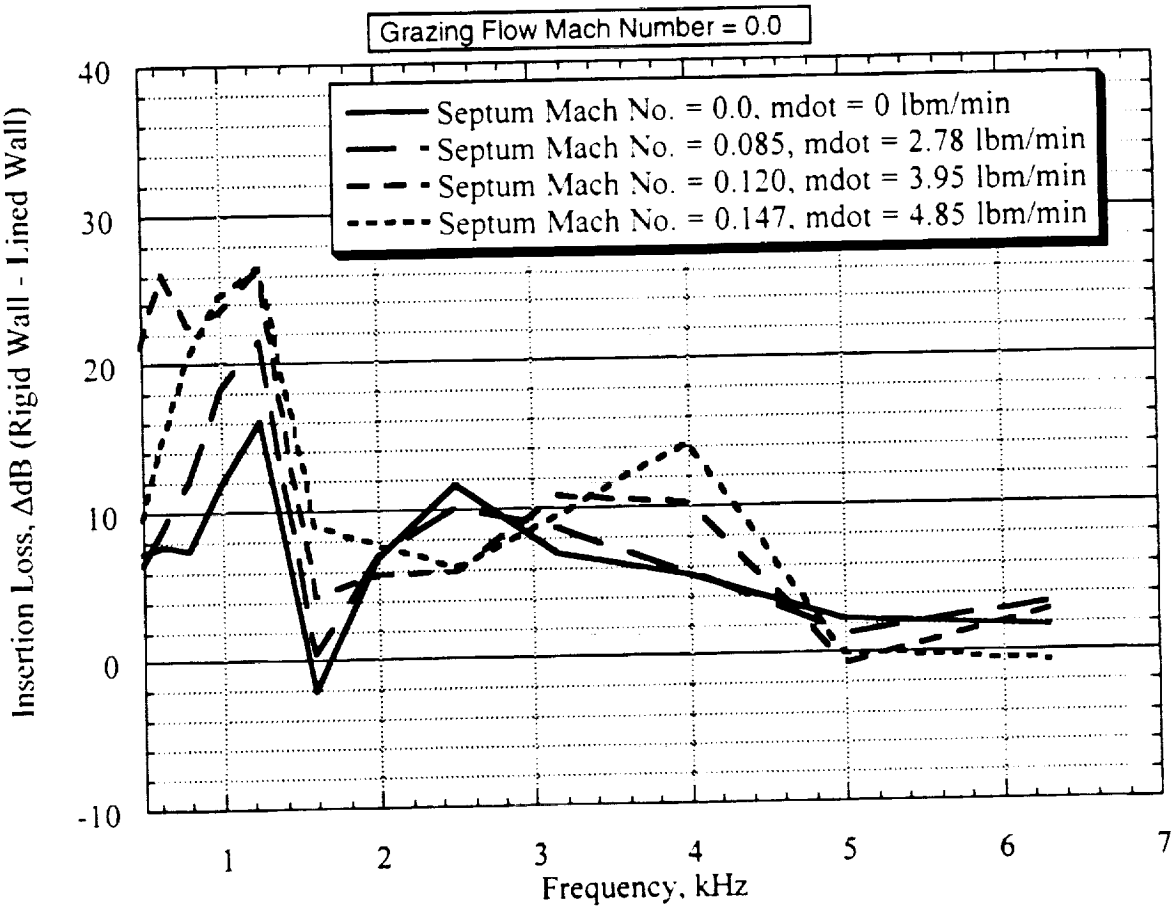

Figure 21. Effect of negative bias Flow on insertion loss at 30° farfield mic with no grazing flow. (500 Hz - 6400 Hz Sweep Input, 64 Avgs, 1/3 Octave Band) Test bs3-bs4

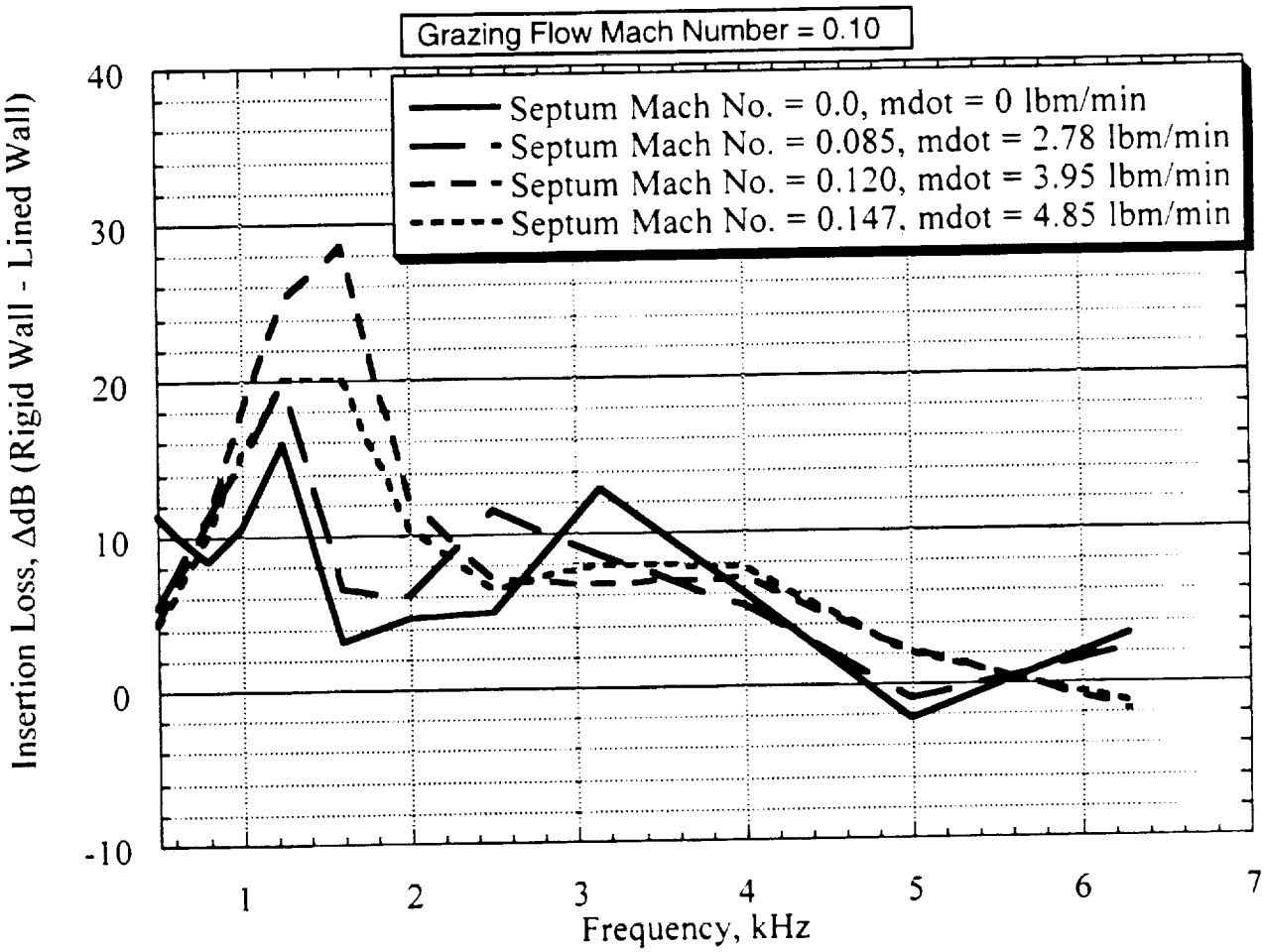

Figure 22. Effect of negative bias flow on insertion Loss at 30° farfield mic
M_{gr} = 0.10 (500 Hz - 6400 Hz Sweep Input, 64 Avgs, 1/3 Octave Band)
Test bs3-bs4

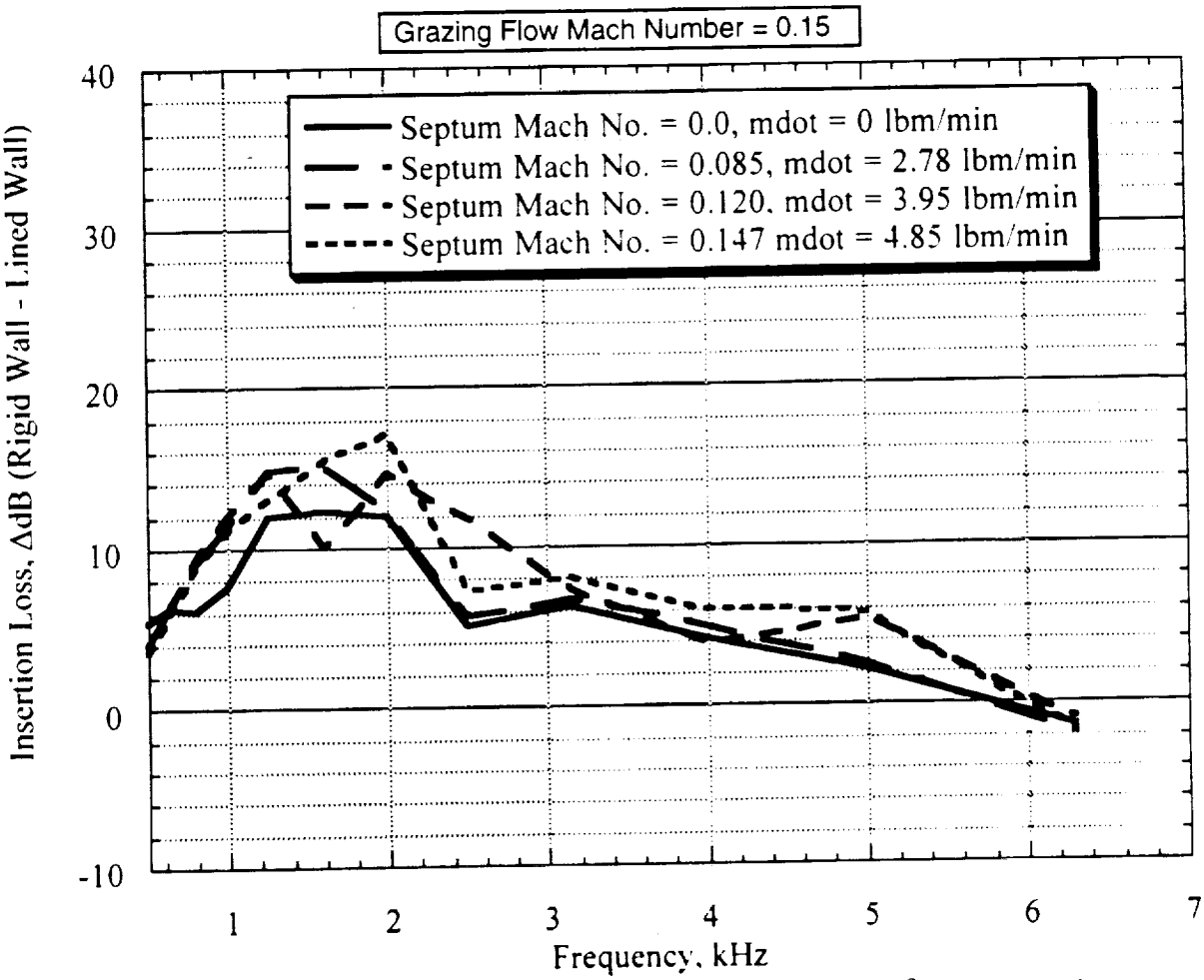

Figure 23. Effect of negative bias flow on insertion loss at 30° Farfield Mic
M_{gr} = 0.15 (500 Hz - 6400 Hz Sweep Input, 64 Avgs, 1/3 Octave Band).
Test bs3-bs4

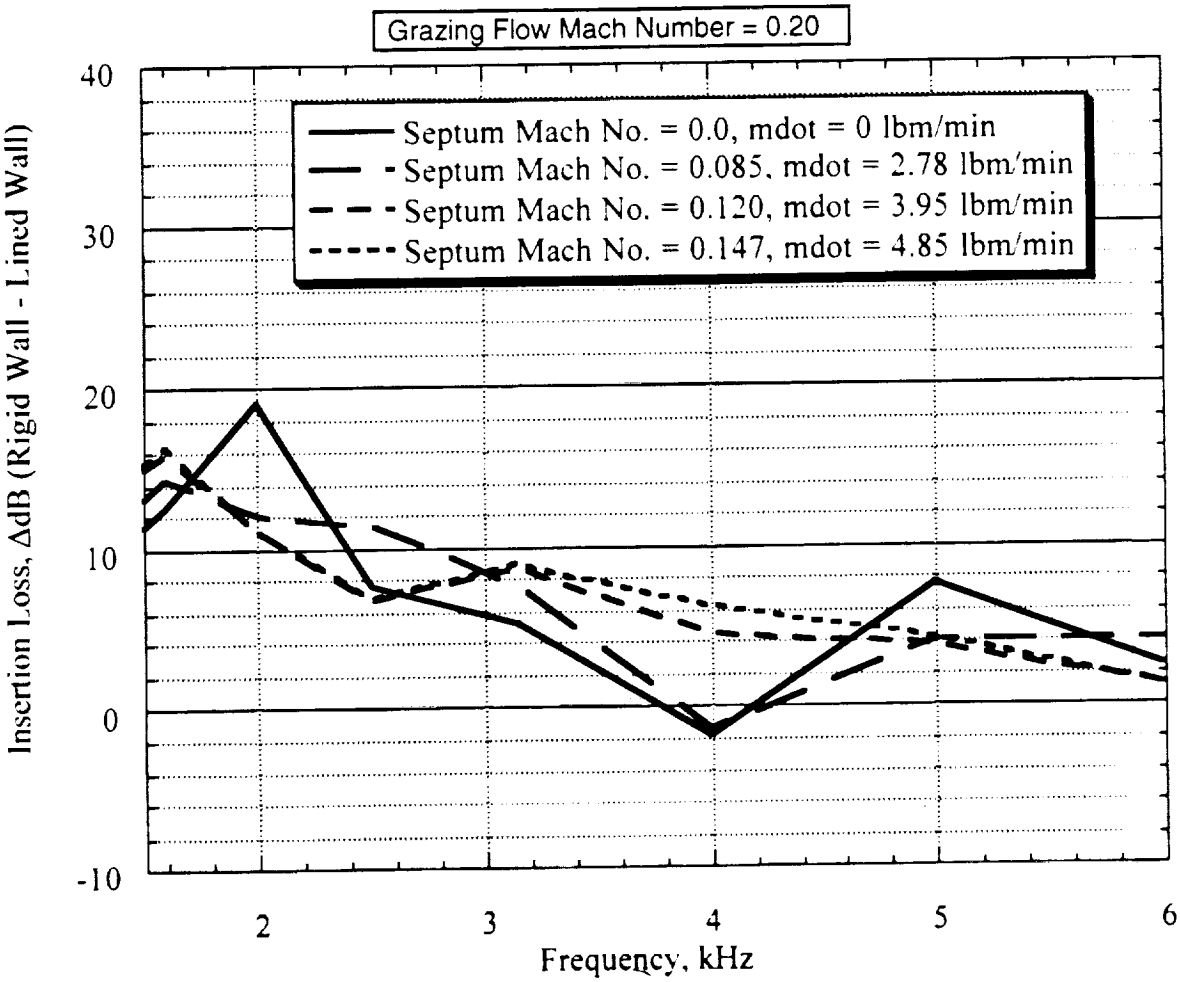

Figure 24. Effect of negative bias flow on insertion loss at 30° farfield mic
M_{gr} = 0.20 (500 Hz - 6400 Hz Sweep Input, 64 Avgs, 1/3 Octave Band)
Test bs3-bs4